Progressive Damage and Failure analysis of Automotive Wheels Using an Explicit Finite Element Method

Mohammed Billal Kamal and Gurumoorthy Sankara Subramania
FCA Engineering India Pvt Ltd

Thomas Oery
FCA US LLC

2016 Science in the Age of Experience, Boston, MA
May 24, 2016

Abstract: *Material degradation and dynamic loadings are the main reasons for the damage in metals. Material degradation was caused by crack initiation and fatigue or dynamic loadings are the source for crack growth. The precise and realistic modeling of inelastic behavior of metals is crucial for solving several problems in engineering fields. To predict the initiation and growth of damage, there are several failure models & theories available presently. In this paper, progressive damage and failure material model using explicit finite element techniques are applied to predict the failure of aluminum alloy .This material model has the ability to predict the damage initiation as a result of ductile and shear failure. Based on the specified damage evolution process, the material stiffness was reduced progressively after the damage initiation. The progressive damage models allow a smooth degradation of the material stiffness, in both quasi-static and dynamic situations. Further in this paper, for tensile and shear failure, the material model was validated for standard specimens. Then the validated material model was adopted in the damage prediction of the aluminum wheel due to compression load and good correlation was achieved within 5% of deviation.*

Keywords: *Progressive damage, Failure model, Damage prediction, Damage initiation, Damage evolution, Crack initiation, Cark propagation, Tensile Failure, Shear Failure, Tensile test, Shear test, Compression test, Wheel damage, Wheel Compression, Wheel spoke loading, Wheel window loading, Explicit*

1. Introduction

In ductile metals, the necking formation takes place initially due to the extensive plastic deformation. Following the necking, the void or crack nucleation will form within the solid and it will grow. Then coalescence of micro voids will occur, which will lead to the separation. Figure 1 shows the crack formation of elongated voids due to elongation and shear by linking up the voids.

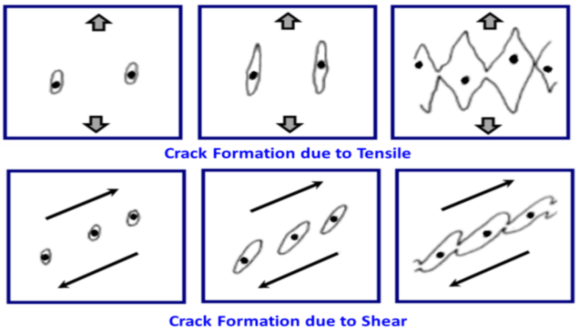

Figure 1. Crack formation

A general structure for material failure modeling allows the combination of multiple failure mechanisms acting at the same time on the material. Material failure refers to the complete loss of load-carrying capacity which results from progressive degradation of the material stiffness. The stiffness degradation process was modeled using damage mechanics.

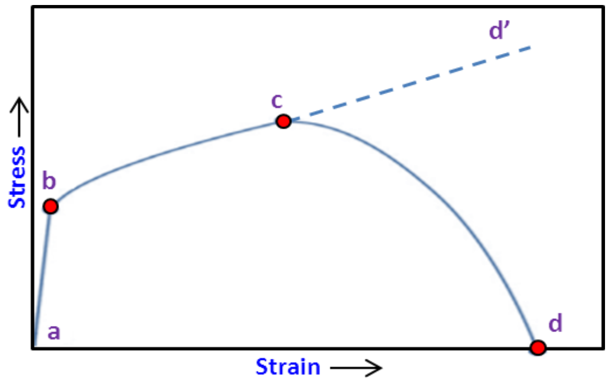

Figure 2. Metals - Uniaxial stress-strain response

The stress-strain response in Figure 2 shows different phases during the uniaxial testing. The material response is initially linear elastic (a-b) followed by plastic yielding with strain hardening (b-c). After the point c, there is an obvious reduction of load-carrying capacity until rupture (c-d). The deformation during this last phase is localized in a neck region of the specimen.

2. Progressive Damage and Failure Model

In Abaqus, the material failure mechanisms is represented in four different parts as shown in Figure 2,

1. The undamaged material response, from points a-b-c-d'.
2. A damage initiation criterion, which starts at point c.
3. A damage evolution, from point c-d.
4. An element deletion, where the elements will be removed from the calculations once the stiffness is fully degraded, i.e. after point d.

2.1 Damage Initiation Criteria for Metal Fracture "(Abaqus,2013)"

The fracture of ductile metals is caused by two failure mechanisms,

1. Ductile fracture due to the nucleation, growth, coalescence of voids.
2. Shear fracture due to the shear band localization.

2.1.1 Ductile criterion "(Abaqus,2013)"

The ductile criterion predicts the onset of damage due to nucleation, growth and coalescence of voids. The model assumes that the equivalent plastic strain at the onset of damage as

$$\bar{\varepsilon}_D^{pl}\,(\eta, \dot{\bar{\varepsilon}}^{pl})$$

where, $\bar{\varepsilon}_D^{pl}$ is a function of stress triaxiality and strain rate. $\eta=-p/q$ is the stress triaxiality, p is the pressure stress, q is the mises equivalent stress, and $\dot{\bar{\varepsilon}}^{pl}$ is the equivalent plastic strain rate.

The criterion for damage initiation is met when the following condition is satisfied:

$$\omega_D = \int \frac{d\,\bar{\varepsilon}^{pl}}{\bar{\varepsilon}_D^{pl}\,(\eta, \dot{\bar{\varepsilon}}^{pl})} = 1\,, \qquad (1)$$

where, ω_D is a state variable that increases monotonically with plastic deformation. At each increment, during the analysis, the incremental increase in ω_D is computed as,

$$\Delta\omega_D = \frac{\Delta\bar{\varepsilon}^{pl}}{\bar{\varepsilon}_D^{pl}\,(\eta, \dot{\bar{\varepsilon}}^{pl})} \geq 0. \qquad (2)$$

2.1.2 Shear criterion "(Abaqus,2013)"

The shear criterion is predicting the onset of damage due to shear band localization. The model assumes that the equivalent plastic strain at the onset of damage,

$$\bar{\varepsilon}_S^{pl}\,(\theta_{s,}\dot{\bar{\varepsilon}}^{pl})$$

where, $\bar{\varepsilon}_S^{pl}$ is a function of the shear stress ratio and strain rate. $\theta_{s,} = (q + k_s\, P)/\tau_{max}$ is the shear stress ratio, $\tau_{max}$is the maximum shear stress, and k_s is the material parameter.

The criterion for damage initiation would occur if the following condition is satisfied,

$$\omega_s = \int . \frac{d\,\bar{\varepsilon}^{pl}}{\bar{\varepsilon}_S^{pl}\,(\theta_{s,}\dot{\bar{\varepsilon}}^{pl})} = 1, \quad (3)$$

where, $\omega_s$is a state variable that increases monotonically with plastic deformation proportional to the incremental change in equivalent plastic strain. At each increment during the analysis the incremental increase in ω_s is computed as,

$$\Delta\omega_s = \frac{\Delta\bar{\varepsilon}^{pl}}{\bar{\varepsilon}_S^{pl}\,(\theta_{s,}\dot{\bar{\varepsilon}}^{pl})} \geq 0. \quad (4)$$

2.2 Damage Evolution "(Abaqus,2013)"

The damage evolution law describes the rate of degradation of the material stiffness once the corresponding initiation criterion has been reached. The degradation of the stiffness associated with each active failure mechanism could be modeled using a scalar damage variable, di. At any given time during the analysis, the stress tensor in the material is given by the scalar damage equation,

$$\sigma = \frac{F}{A} \text{ and } \bar{\sigma} = \frac{F}{A - A_D}$$

$$\bar{\sigma} = \frac{F}{A(1-\frac{A_D}{A})} \text{ , where } D = \frac{A_D}{A}$$

$$\sigma = (1 - D)\bar{\sigma} \quad (5)$$

where, D is the overall damage variable, σ is the true stress, $\bar{\sigma}$ is the effective or undamaged stress, A is original surface area and A_D is defects surface area.

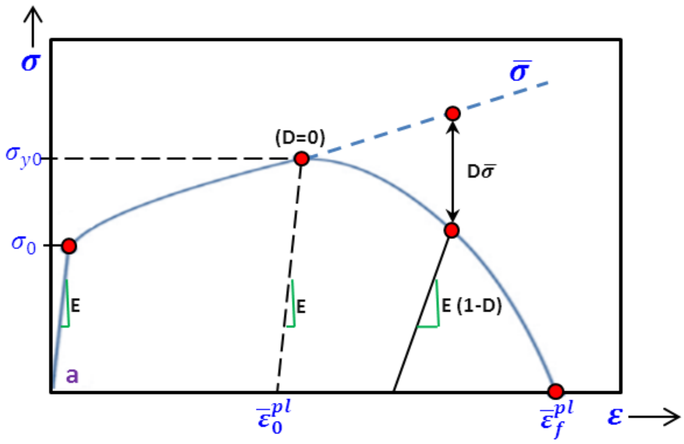

Figure 3. Metal - Stress-strain curve with progressive damage degradation

In Figure 3, E is Young's modulus, σ_{y0} and $\bar{\varepsilon}_0^{pl}$ are yield stress and equivalent plastic strain at the onset of damage, $\bar{\varepsilon}_f^{pl}$ is the equivalent plastic strain at failure (when the D=1). The material would lose its load carrying capacity once the D=1. The element would be removed from the mesh if all of the section points at any one integration location lose their load-carrying capacity.

2.2.1 Damage Evolution based on Effective Plastic Displacement "(Abaqus,2013)"

Once the damage initiation criterion is reached, the effective plastic displacement, $\bar{u}^{pl}$, is defined with the evolution equation,

$$\dot{\bar{u}}^{pl} = L\,\dot{\bar{\varepsilon}}^{pl}, \qquad (6)$$

where, L is the characteristic length of the element and $\dot{\bar{\varepsilon}}^{pl}$ is effective plastic strain.

The evolution of the damage variable with the relative plastic displacement could be specified in tabular, linear, or exponential forms. The linear form of damage evolution with plastic displacement is

$$\dot{d} = \frac{L\,\dot{\bar{\varepsilon}}^{pl}}{\bar{u}_f^{pl}} = \frac{\dot{\bar{u}}^{pl}}{\bar{u}_f^{pl}}, \qquad (7)$$

If $\bar{u}^{pl} = \bar{u}_f^{pl}$, then the material stiffness will be fully degraded (d=1).

2.2.2 Damage Evolution based on Energy Dissipation "(Abaqus,2013)"

The fracture energy per unit area, G_f, is the energy dissipated during the damage process directly. Instantaneous failure would occur if G_f is specified as 0.

The linear form of damage evolution with plastic displacement is

$$\dot{d} = \frac{L\,\dot{\bar{\varepsilon}}^{pl}}{\bar{u}_f^{pl}} = \frac{\dot{\bar{u}}^{pl}}{\bar{u}_f^{pl}}, \qquad (8)$$

where the equivalent plastic displacement at failure is calculated as

$$\bar{u}_f^{pl} = \frac{2\,G_f}{\sigma_{y0}}, \qquad (9)$$

where σ_{y0} is the yield stress at the time when the failure criterion is reached.

3. Numerical Model Validation

The damage material model is validated with the simple tensile, shear and compression test results. The test specimens were made from the cast aluminum wheel casting. The computer aided engineering (CAE) results showed a good agreement with the tensile, shear and compression test results for the failure mode and the strength values.

3.1 Material Model

The plastic property from the true stress strain curve for the aluminum is defined till the point of the damage initiation and after this point the plastic property is raised linearly. The damage initiation is defined using the plastic strain which is obtained from the material's stress-strain data. The damage evolution is defined using the energy data.

3.2 Tensile Test

In CAE, the tensile specimen was meshed using the hexahedral elements and the behavior was studied with different mesh sizes. One end of the tensile specimen was fixed and enforced displacement was applied on the other end till the failure. A tensile test study was done for different material models in CAE to study how the damage initiation criterion and the damage evolution work in the progressive damage model. After the yield, the linear model continued the elastic slope, and after the breaking strain limit, the plasticity model continued the slope before the ultimate limit. In progressive damage material model, the stiffness was reduced after the ultimate limit. Figure 4 shows the comparison between the stress-strain curves of the tensile specimen from the CAE results for different material models.

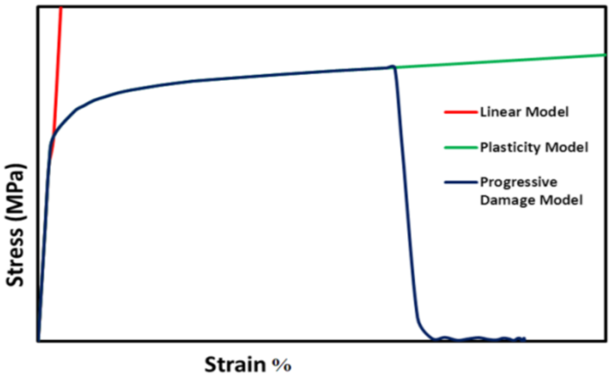

Figure 4. Comparison between Linear, Plasticity and Progressive damage material models

Figure 5 shows the deformation behavior of the tensile specimen in CAE. Figure 6 shows the force vs deflection (FD) curve from the tensile test simulation and the comparison of the tensile strength value from the test and CAE results. The CAE tensile strength was calculated by dividing the tensile force by the cross sectional area of the specimen. The failure mode and tensile strength value calculated from the CAE was close to the test results within 6% of deviation.

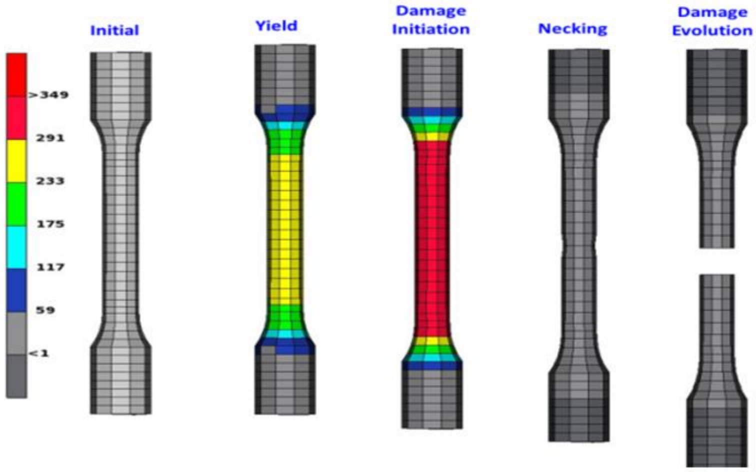

Figure 5. Stress plot and deformation behavior of the specimen in tensile test

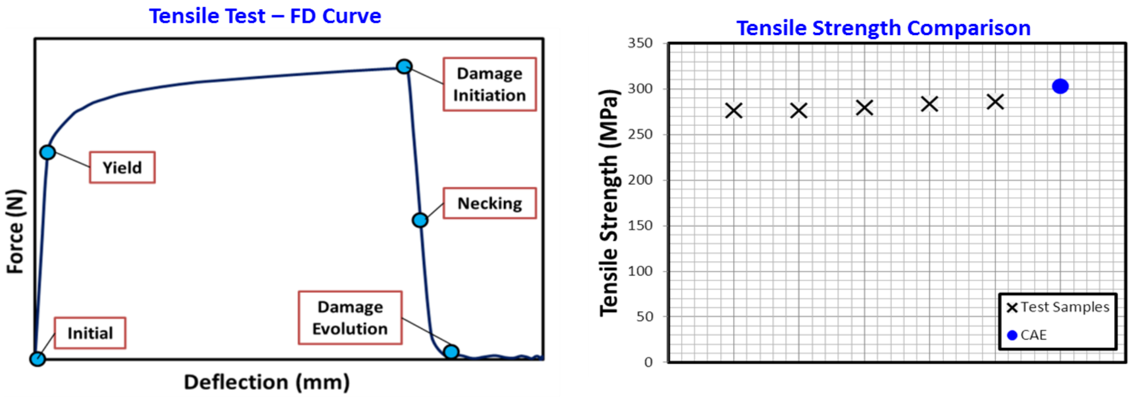

Figure 6. Specimen Tensile Test Results and Comparison

The material exhibits strain-softening behavior that would lead to strain localization. This formulation leads to a mesh dependency of the finite element results, where the energy dissipated decreases upon mesh refinement. To check the result variation due to the element's size, the tensile test was performed for three different mesh sizes like 1mm, 2mm and 4mm. The stress value calculated for the 1mm mesh was close to the test results within 2.8% of deviation and the stress values for the 4mm mesh deviated around 6% when compared to the test results. Figure 7 shows the meshed models of the tensile specimen and the stress-strain comparison between the test and CAE results of different mesh sizes.

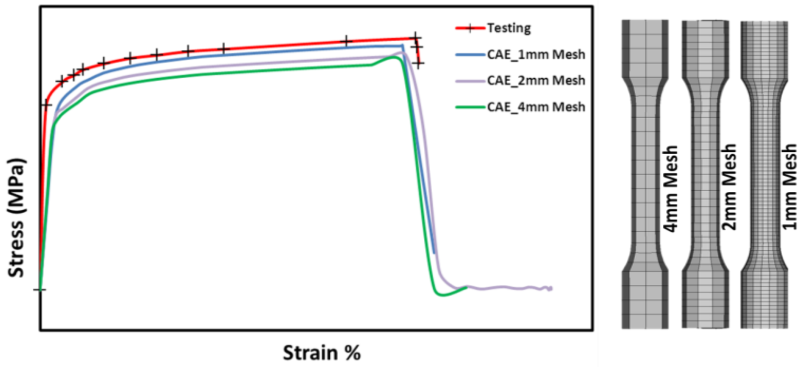

Figure 7. CAE results comparison: Different mesh size

3.3 Compression Test

The compressive specimen was meshed using the hexahedral elements with the average element size of 1mm. The compressive specimen was placed between the top and bottom rigid plates. The bottom plate was fixed and compressive load was applied through the top plate until the failure of the specimen. Figure 8 shows the loading set-up and the compressive strength prediction from testing and CAE results. The prediction of CAE results was close to the test results within 7% of deviation.

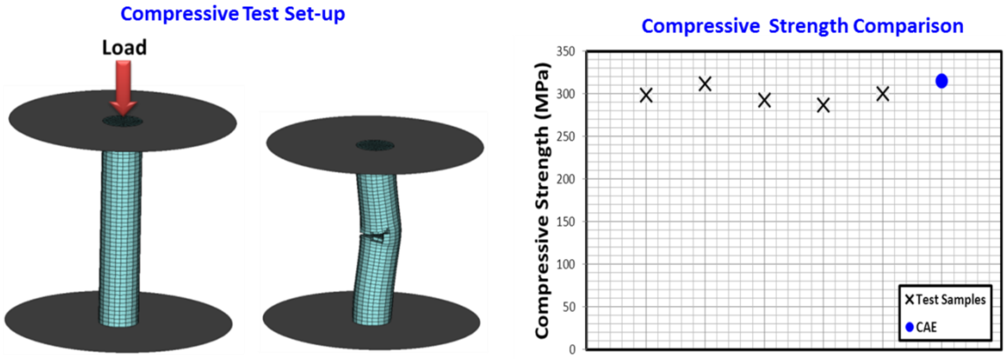

Figure 8. CAE Compressive Test Step-up and Comparison (Test Vs CAE)

3.4 Shear Test

The shear specimen was meshed using the hexahedral elements with the average element size of 1mm. The specimen was placed in the hole between the two rigid fixtures. The bottom fixture was fixed and the top fixture was moved upward until failure of the specimen. Figure 9 shows the loading set-up and the shear strength prediction from testing and CAE results. The prediction of CAE results was close to the test results within 5% of deviation.

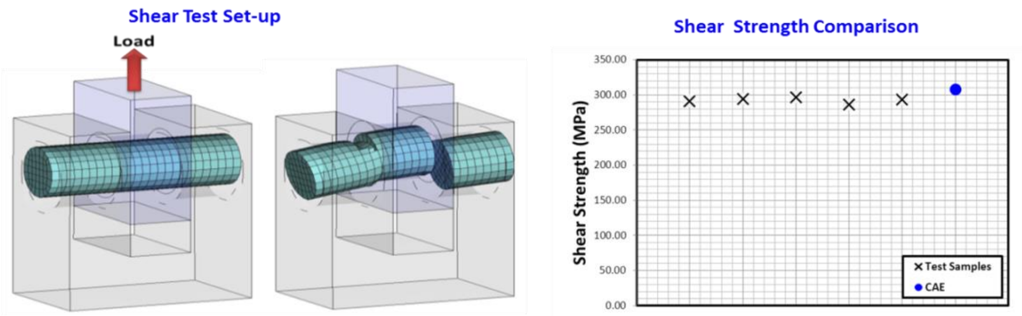

Figure 9. CAE - Shear Test Step-up and Comparison (Test Vs CAE)

4. Wheel Compressive Load Prediction

The aluminum wheel compression test studies the wheel's compressive failure mode and load at failure, which is useful for the wheel design to meet the strength and the safety requirements. Figure 10 shows the schematic setup of the wheel compressive test. The wheel was placed between the fixed and movable rigid applicator and the wheel was compressed by the movable applicator until the major damage occurred in the wheel.

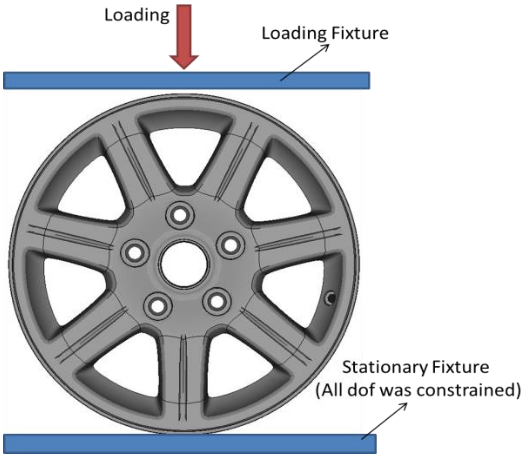

Figure 10. Wheel compression - Test setup

4.1 Damage prediction for 17" Wheel

The wheel was meshed using the hexahedral element with 4mm mesh size. The non-linear plastic material was defied to represent the stress-strain behavior and progressive damage material model was used to predict the damage behavior. All Degree Of Freedom (DOF) in stationary fixture was constrained and the compressive load was applied through the rigid applicator. The general contact was used by considering all interior and exterior element faces. The Abaqus explicit solver was used for this simulation. Figure 11 shows the CAE compressive test results and Figure 12 shows the FD curve for the 17" wheel compressive test.

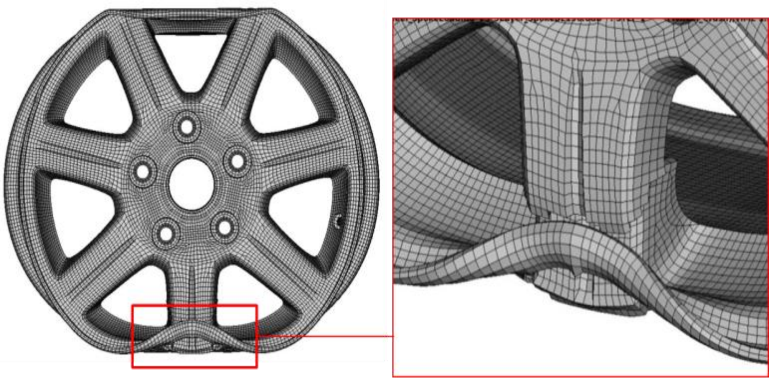

Figure 11. 17" Wheel CAE results: Deformation plots

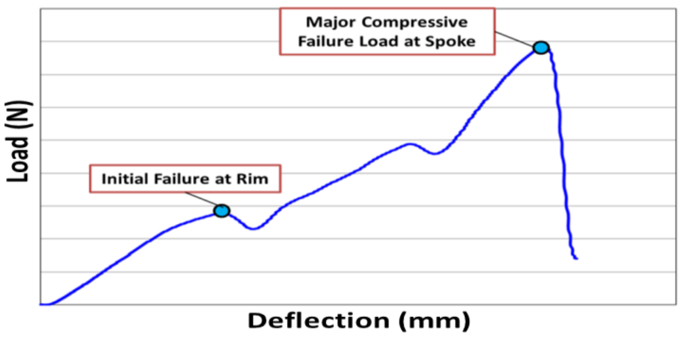

Figure 12. 17" Wheel: CAE FD curve

The initial damage occurred at the top and bottom of the rim regions, and then the load transferred to the spokes where the major damage occurred. Figure 13 shows the damage initiation criterion plots, which indicates that the initiation of the damage (Ductile damage initiation, ω_D / Shear damage initiation, ω_s). Figure 14 shows the stiffness degradation plots (D_{max}), which indicates that the elements will be deleted once the maximum degradation value was reached 1.0 (D_{max}=1.0).

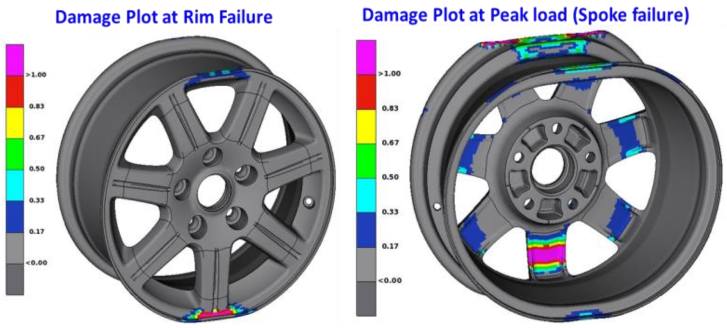

Figure 13. 17” Wheel CAE results: Damage initiation criterion plots

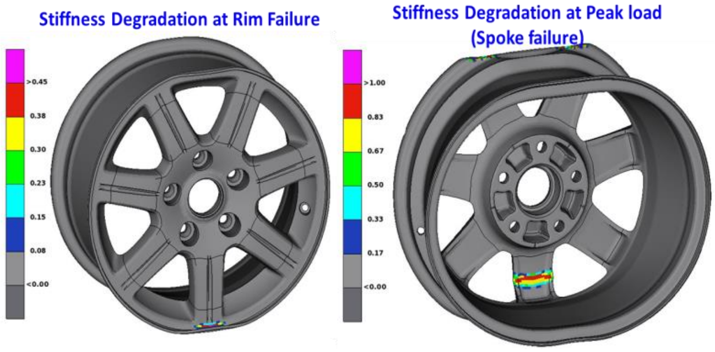

Figure 14. 17” Wheel CAE results: Overall stiffness degradation (D) plots

4.1.1 Test Correlation

Figure 15 shows the 17” wheel damage after the lab testing and CAE results, it also shows the FD curve comparison between the lab and CAE results. The CAE curve trend and the maximum compressive load, matched with the test results within a 5% deviation.

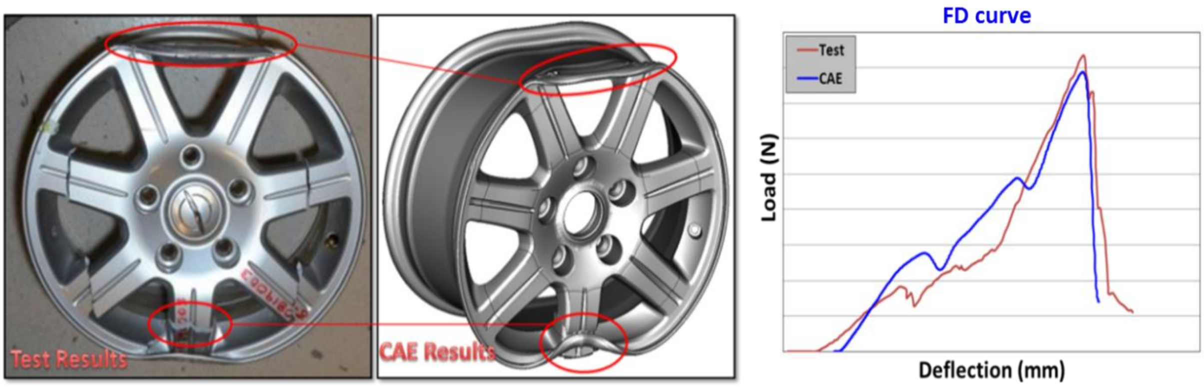

Figure 15. 17” Wheel damage: Comparison between Lab test and CAE

4.2 Damage prediction for 19” Wheel

The major damage occurred during the wheel compressive test in spoke or hub regions, which mainly depended on the wheel designs. Figure 16 shows the wheel damage study for the 19” wheel, where the major damage occurred in the hub region. The loads were applied at the spoke (spoke loading) and between the spokes (window loading). At peak load the major damage was found on the hub region for both the spoke and window loadings. Figure 17 shows the wheel damage comparison between the lab test and CAE results for the spoke loading. The damage location prediction in the CAE was similar to test results and the peak compressive load prediction in CAE was within 4% of deviation from the lab test results.

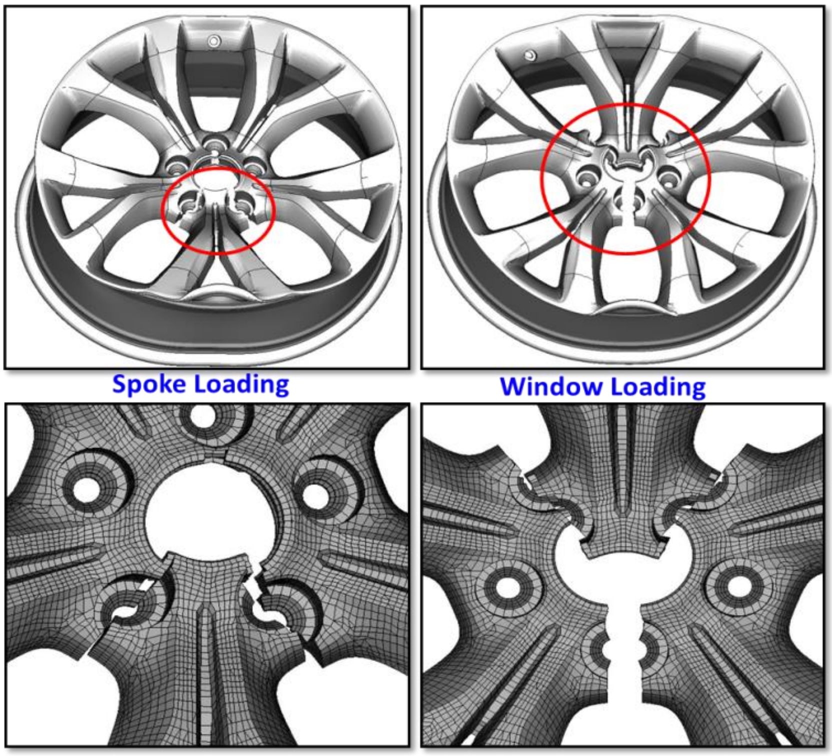

Figure 16. 19” Wheel damage prediction at Hub region

Figure 17. 19” Wheel Damage: Comparison between Lab test and CAE results for spoke loading

5. Conclusions

In this paper, the procedure for the damage prediction of the metals using the progressive damage and failure material model is presented. The conventional elastic – plastic material model was useful for predicting the failure at the ultimate stress state. However after this state also, the components possess the load carrying capacity changing the failure region. The progressive damage model using ductile and shear failure criteria was useful to predict the failure load and failure modes. The simple specimen tests like tensile, compressive and shear tests were useful and more confidence was gained related to material model validation. The major damage location was identified and peak load at failure for wheels was obtained from the CAE results. A good correlation was achieved between CAE and the lab test results. Using the validated material model and simulation method, the component failure load and the failure modes could be predicted at early stages of the design.

6. References

1. K Billal, M., Basha, R., Nesarikar, A., Haiyum, A. et al., "Prediction of Component Failure using ‘Progressive Damage and Failure Model’ and Its Application in Automotive Wheel Design," SAE Technical Paper 2015-01-1516, 2015, doi:10.4271/2015-01- 1516.
2. Abaqus User's Manual 6.13 Version, 2013.
3. Thairy H. AL , Wang Y C, “A Numerical Study of the Behavior and Failure Modes of Axially Compressed Steel Columns Subjected to Transverse Impact”, International Journal of Impact Engineering, 2011,
4. Michael Brunig, Oliver Chyra, Daniel Albrecht, Larissa Driemeier, Marcı´lio Alves, “ A ductile damage criterion at various stress tri axialities”, International Journal of Plasticity 24 (2008)
5. Werner H, Hooputra H, Weyer S, Gese H, "Applications of phenomenological failure models in automotive crash simulations", VIII International Conference on Computational Plasticity, Barcelona, 2005.
6. Andrea Ockewitz, Dong-Zhi Sun, Herbert Klamser, Daniel Malcher, " Damage Modelling of Automobile Components of Aluminium Materials under Crash Loading", LS-Dyna Anwendreforum, Ulm 2006.